Portland State University
PDXScholar

Chemistry Faculty Publications and Presentations   Chemistry

2008

Chiral Recognition of Amino Acids by Use of a Fluorescent Resorcinarene

Gerald I. Richard
Louisiana State University

Hadi M. Marwani
Louisiana State University

Shan Jiang
Louisiana State University

Sayo O. Fakayode
Winston-Salem State University

Mark Lowry
Louisiana State University

See next page for additional authors

Let us know how access to this document benefits you.

Follow this and additional works at: http://pdxscholar.library.pdx.edu/chem_fac

Part of the Biochemistry Commons, and the Chemistry Commons

Authors

Gerald I. Richard, Hadi M. Marwani, Shan Jiang, Sayo O. Fakayode, Mark Lowry, Robert M. Strongin, and Isiah M. Warner

Chiral Recognition of Amino Acids by Use of a Fluorescent Resorcinarene

GERALD I. RICHARD, **HADI M. MARWANI**, **SHAN JIANG**, **SAYO O. FAKAYODE**, **MARK LOWRY**, **ROBERT M. STRONGIN**[*], and **ISIAH M. WARNER**[*]
Department of Chemistry, Louisiana State University, Baton Rouge, Louisiana 70803 (G.I.R., H.M.M., S.J., M.L., I.M.W.); Department of Chemistry, King Abdulaziz University, Jeddah, Saudi Arabia 21589 (H.M.M.); Department of Chemistry, Winston-Salem State University, Winston-Salem, North Carolina 27110 (S.O.F.); and Department of Chemistry, Portland State University, Portland, Oregon 97207 (R.M.S.)

Abstract

The spectroscopic properties of a chiral boronic acid based resorcinarene macrocycle employed for chiral analysis were investigated. Specifically, the emission and excitation characteristics of tetraarylboronate resorcinarene macrocycle (TBRM) and its quantum yield were evaluated. The chiral selector TBRM was investigated as a chiral reagent for the enantiomeric discrimination of amino acids using steady-state fluorescence spectroscopy. Chiral recognition of amino acids in the presence of the macrocycle was based on diastereomeric complexes. Results demonstrated that TBRM had better chiral discrimination ability for lysine as compared to the other amino acids. Partial least squares regression modeling (PLS-1) of spectral data for macrocycle-lysine guest-host complexes was used to correlate the changes in the fluorescence emission for a set of calibration samples consisting of TBRM in the presence of varying enantiomeric compositions of lysine. In addition, validation studies were performed using an independently prepared set of samples with different enantiomeric compositions of lysine. The results of multivariate regression modeling indicated good prediction ability of lysine, which was confirmed by a root mean square percent relative error (RMS%RE) of 5.8%.

Keywords

Chiral analysis; Fluorescent sensors; Chemometrics; Partial least squares regression modeling; PLS-1

INTRODUCTION

Chiral recognition has an important influence on biological systems due to the many naturally occurring chiral molecules such as carbohydrates, amino acids, proteins, hormones, enzymes, and DNA.[1-6] In fact, several biological functions are based on chiral interactions. For example, since human odor receptors are chiral, humans are able to recognize that (*R*)-limonene smells like lemons and (*S*)-limonene smells like oranges. Likewise, D-asparagine tastes sweet and L-asparagine tastes bitter. While it is generally accepted that biological systems are primarily composed of L-amino acids and D-carbohydrates, the presence of D-amino acids at low levels has been reported in humans.[7-10] In addition, D-amino acids may possibly have an antagonistic biological function.

---

*Authors to whom correspondence should be sent. E-mail: iwarner@lsu.edu and strongin@pdx.edu..

The true importance of chirality to human functions was realized in the 1960s when the chiral drug thalidomide was prescribed to pregnant women to alleviate morning sickness. It was later discovered that the (R)-enantiomer produced the desired therapeutic effect, while the (S)-enantiomer resulted in severe birth defects.[11] As a result, there has been a proliferation of studies of enantiomeric selectivity in biological systems, and a concomitant series of analytical methods have been applied. The most commonly used analytical methods involve chromatographic techniques such as high-performance liquid chromatography (HPLC),[12] gas chromatography (GC),[13] and capillary electrophoresis (CE).[14] However, spectroscopic techniques such as UV-visible,[15] nuclear magnetic resonance (NMR),[16] and mass spectroscopy[17] have shown considerable promise in studying chiral recognition ability for different applications. Fluorescence spectroscopy is one of the most powerful and widely used methods in studying the enantioselectivity of several biological systems because of its relatively high sensitivity, selectivity, and versatility.[18-21] Consequently, enantioselective fluorescent sensors have attracted considerable interest for use in potential bioanalytical applications.[22-24]

When enantioselective studies are performed in an achiral environment, chiral discrimination is not observed. Therefore, the use of a chiral selector for chiral recognition of enantiomers is required. For instance, some commonly used fluorescent chiral selectors for spectroscopic investigations of chiral molecules include fluorescent-labeled cyclodextrins,[22] crown ethers,[23] and calixarenes.[24] Previously, a chiral pinanediolderived boronate resorcinarene macrocycle was developed by Lewis et al.[25] Resorcinarenes are cyclic aromatic tetramers synthesized in a single step from an acid catalyzed condensation reaction of resorcinol and an aldehyde.[26] Lewis et al.,[27] He et al.,[28] Davis et al.,[29] and Zhang et al.[30] have previously reported the use of boronic acid based resorcinarene macrocycles for achiral and chiral carbohydrate recognition and chemical sensing using UV-visible spectroscopic methods. Consequently, these macrocycles could be useful in investigating the fluorescence detection and enantiodiscrimination of amino acids.

Amino acids, which are structurally similar to one another, but have different side chains, are among the most important molecules in biological systems because they are also constituents of peptides, proteins, and DNA. Most amino acids exhibit transparency in the UV-visible region. In fact, the optical detection of amino acids has been the focus of several research studies. However, a majority of fluorescent chiral recognition studies involving amino acids have been performed with amino acid derivatives.[31-33] Therefore, fluorescence enantioselective recognition of unmodified amino acids would be an attractive approach for monitoring diseases and understanding protein biological functions. In addition, many approaches have recently demonstrated that the enantiomeric composition of chiral molecules can be determined by multivariate regression modeling of fluorescence emission spectral data.[18,34-36] These results from spectral data measurements have demonstrated that multivariate regression modeling is a reliable method for evaluating the chiral recognition ability of chiral molecules.

This study reports the fluorescent spectral properties of tetraarylboronate resorcinarene macrocycle (TBRM) and investigates the enantiomeric selectivity of unmodified amino acids with TBRM employed as a chiral selector. In addition, the chiral recognition ability of TBRM with selected amino acids as well as determination of enantiomeric composition of lysine was evaluated by use of steady-state fluorescence spectroscopy and multivariate regression analysis.

EXPERIMENTAL

Materials

D- and L-enantiomers of alanine, arginine, asparagine, aspartate, glutamine, glutamate, isoleucine, leucine, lysine, methionine, proline, serine, threonine, and valine were obtained from Sigma-Aldrich (St. Louis, MO) and used as received. Spectroscopic grade (≥99.9%) acetonitrile, dimethyl sulfoxide, ethyl acetate, methanol, and tetrahydrofuran were also purchased from Sigma Aldrich (St. Louis, MO) and used as received. Resorcinol, 4-formylphenylboronic acid, ethanol, hydrochloric acid, dimethyl formamide, sodium sulfate, and 1R, 2R, 3S, and 5R-(-)-pinanediol were obtained from Sigma Chemical Company (Milwaukee, WI). The purity of all analytes and reagents was 99% or higher.

Tetraarylboronate Resorcinarene Macrocycle Synthesis

The chiral (-)-pinanediol tetraarylboronate resorcinarene (72% yield) macrocycle (Fig. 1) was synthesized according to the procedure described by Lewis et al.[25] The structure of the synthesized TBRM was confirmed by NMR.

Sample Preparation

Stock solutions of TBRM in spectroscopic grade methanol and each amino acid in carbonate buffer (pH 7.2) were prepared. For the polarity study, an individual standard solution of the chiral macrocycle (7 μM) was prepared in different solvents. In addition, a series of different standard solutions of TBRM were prepared in methanol for determining the fluorescence quantum yield of the chiral macrocycle. For the enantiomeric selectivity of amino acids, mixtures of chiral macrocycle (7 μM) and amino acid (1 mM) were also prepared in methanol (90%) and water (10%). All standard solutions were made in triplicate. For chemometrics experiments, a stock solution containing 50 μM of TBRM was prepared in methanol. Twenty mM stock solutions of each lysine enantiomer were prepared in carbonate buffer (pH 7.2). From the stock solutions, the final concentration of all calibration and validation solutions contained fixed macrocycle (7 μM) and amino acid (2 mM) enantiomer concentrations. The enantiomeric composition of the calibration samples ranged from 0.1 to 1.0 mole fraction while the validation samples ranged from 0.05 to 0.95 mole fraction.

Data Analysis

Multivariate data analysis was achieved using the Unscrambler™ (version 9.1; CAMO, Inc., Corvalis, OR). Partial least squares regression models (PLS-1) were developed from the spectral data of guest-host complexes using full cross-validation. The models were validated with independently prepared test solutions containing known mole ratios of lysine.

Instrumentation

Steady-state fluorescence measurements were performed in triplicate at room temperature using a Spex Fluorolog-3 spectrofluorometer (model FL3-22TAU3, Jobin Yvon, Edison, NJ) equipped with a 450 W xenon lamp, double grating excitation and emission monochromators, and an R928P photomultiplier tube detector. Excitation and emission spectra were acquired using a 10 mm quartz fluorometer cell with excitation bandpass set at 1 nm and emission bandpass at 4 nm. The excitation and emission wavelengths were monitored at 290 and 435 nm, respectively, for the chiral macrocycle. In addition, absorbance measurements were made in triplicate at room temperature using a UV-3101 PC (UV-VIS NIR) scanning spectrophotometer (Shimadzu, Columbia, MD) equipped with a deuterium halogen lamp. The absorbance spectra were recorded in 10 mm quartz cells. Both fluorescence and absorption spectra were blank subtracted before proceeding with the data analysis.

RESULTS AND DISCUSSION

TBRM Spectroscopic Characteristics

Fluorescence spectroscopic properties, including emission and excitation characteristics and quantum yield of TBRM, were investigated. The influence of different solvents on the chiral macrocycle's microenvironment was evaluated. Different spectroscopic grade solvents, including acetonitrile, dimethyl sulfoxide (DMSO), ethyl acetate, methanol, and tetrahydrofuran, were used in order to study the fluorescence characteristics of TBRM. Significant shifts in fluorescence spectra of the chiral macrocycle in the presence of each solvent were observed at the maximum emission wavelength. The TBRM maximum emission wavelengths in tetrahydrofuran, ethyl acetate, acetonitrile, DMSO, and methanol were 325, 350, 390, 410, and 435 nm, respectively. In general, these marked shifts in the maximum emission wavelength are indicative of non-covalent interactions between the solvent molecules and the chiral macrocycle.

The quantum yield of the TBRM was determined in order to evaluate its fluorescence efficiency. For determination of the TBRM fluorescence quantum yield, L-tryptophan (L-Trp) was selected as a standard sample since L-Trp absorbs near the excitation wavelength ($\lambda_{\mathrm{max\ ex}} = 290$ nm) of the chiral macrocycle. As a result, it is expected that the same number of photons will be absorbed by both samples. Dilute solutions of TBRM (1-10 µM) and L-Trp (4-22 µM) were prepared in methanol and water, respectively. The fluorescence of the standard and unknown were recorded using the same standard and unknown solutions used for absorbance measurements.

The quantum yield of the chiral macrocycle was calculated using the following equation:[37]

$$\Phi_x = \Phi_{\mathrm{std}}\left(Grad_x / Grad_{\mathrm{std}}\right)\left(\eta_x^2 / \eta_{\mathrm{std}}^2\right)$$

(1)

where the x and std subscripts denote the chiral macrocycle (unknown) and L-Trp (used as the standard), respectively, Φ is the quantum yield, $Grad$ is the slope from the plot of integrated fluorescence intensity versus absorbance, and η is the refractive index. The quantum yield of L-Trp has been previously reported in water as 0.14.[38] The refractive indices for water and methanol are 1.32 and 1.33, respectively. Using Eq. 1, the calculated quantum yield of TBRM at a maximum emission wavelength of 435 nm was 0.10, indicative of a relatively highly fluorescence efficient macrocycle.

Amino Acid Chiral Recognition

The enantiomeric selectivity of the chiral macrocycle towards different amino acids was examined. Spectral differences of TBRM (7 µM) with the investigated amino acids (1 mM) were obtained as illustrated in Fig. 2. Fluorescence intensity (ΔI) was acquired by subtracting the emission peak of TBRM from that of the TBRM and amino acid mixture at 435 nm. In general, it was observed that the fluorescence intensity of the macrocycle was higher in the presence of L-amino acid enantiomers as compared to D-amino acids. This is indicative of the higher enantiomeric selectivity of the TBRM towards L-amino acids in contrast to D-amino acids. However, the opposite trend was observed in the fluorescence intensity for TBRM with L-arginine, L-glutamate, and L-proline. Interestingly, the difference in the fluorescence intensity of the macrocycle in the presence of D- and L-lysine was the highest compared to all the investigated amino acids.

Various degrees of enantioselectivity for amino acids were observed, as illustrated in Fig. 2. The chiral recognition of amino acids is based on the formation of diastereomeric complexes

between the enantiomer and the chiral macrocycle, as indicated by differences in the fluorescence emission of TBRM with amino acid enantiomers. It is observed that there were significant differences in fluorescence intensity of TBRM with alanine, leucine, and lysine enantiomers as compared to less evident changes for arginine, aspartate, and asparagine enantiomers. Moreover, all amino acids used in this study do not absorb in the same region as the chiral macrocycle, further supporting the idea that the changes in fluorescence intensity were due to interactions between the macrocycle and amino acid enantiomers.

As noted above, the enantiomeric selectivity of the macrocycle was the highest towards L-lysine (L-Lys) as compared to all other amino acids investigated. This high chiral recognition ability of TBRM for lysine can be attributed to the excitation spectra of the macrocycle with lysine in which there is not only a peak at 290 nm but also a peak at 350 nm (Fig. 3A), suggesting complex formation with TBRM and lysine. At 290 nm, the excitation intensity of TBRM is decreased in the presence of D-Lys, while it is increased in the presence of L-Lys. However, at 350 nm the excitation intensity of TBRM with L-Lys is higher than that of TBRM with D-Lys. An excitation peak around 350 nm was not observed in the spectrum of TBRM with any other amino acids investigated. The peak at 350 nm was investigated by collecting the emission at an excitation of 350 nm (Figure 3B). As a result, no fluorescence emission was observed for the macrocycle in the absence of amino acid at this excitation wavelength. For the macrocycle and D-Lys (or L-Lys) mixture, however, an emission spectrum with a maximum fluorescence intensity at 420 nm was observed. In addition, the emission intensity of the macrocycle with L-Lys was higher than that with D-Lys.

Determination of Enantiomeric Composition

Accurate determination of the enantiomeric composition of amino acids is important, particularly for the pharmaceutical industry, because D-amino acids have been detected at low concentrations in humans, which may have an antagonistic biological function. In addition, deficiencies in L-lysine concentrations have been reported to result in mental retardation and hyperammonemia.[39,40] However, an increase in L-lysine concentrations can prevent the recurrence of herpes simplex infections.[41]

In this phase of our study, fluorescence steady-state-based measurements were used to determine the enantiomeric composition of chiral molecules. This investigation was performed for screening purposes and as a proof of principal for this fluorescence approach. Relatively high concentrations of amino acids were employed. However, it is expected that the concentrations could be significantly reduced upon further optimization. As previously noted, the enantiomeric selectivity of the chiral macrocycle was highest with lysine as compared to other amino acids. To further understand the chiral recognition ability of the chiral macrocycle towards lysine, determination of the enantiomeric composition was investigated for lysine using partial least squares regression modeling (PLS-1). In fact, multivariate regression modeling allows quick and accurate screening of chiral molecules, and it has been widely used for correlating spectral variations with known compositional changes.[18,34,35,42] According to procedures from previous studies, PLS-1 regression modeling was used to correlate changes in spectral data of guest-host complexes with enantiomeric composition of samples.

Figure 4A illustrates the emission spectra of different mixtures containing a fixed concentration of the macrocycle (7 μM) and lysine (2 mM) with varying the enantiomeric composition of lysine. The samples have a maximum emission at 420 nm. Spectral variations of the macrocycle were observed with different enantiomeric compositions of lysine. Again, this finding is indicative of the formation of diastereomers in the different samples. In addition, this is further confirmed by a mean-centered plot (Fig. 4B) obtained by averaging the spectral data of the mixtures (Fig. 4A) and subsequently subtracting the average spectrum from each individual sample spectrum on a wavelength-by-wavelength basis.[18] Mean-centered plots offer better

insight into the spectral variations of TBRM that occurred with different enantiomeric compositions of lysine. It is also interesting to note that the spectral data of samples with enantiomeric compositions of L-Lys greater than 0.5 mol fractions are above the plot's origin, while those with mol fractions less than 0.5 are below the origin, as illustrated in Fig. 4B.

The above findings are also supported by multivariate regression methods. From PLS-1, the correlation coefficient (0.9932), the slope (1.0158), and the offset (0.0168) were obtained from the calibration regression modeling. A perfect model would have a correlation coefficient of 1, a slope of 1, and an offset of 0. The results of the actual mole ratio, predicted mole ratio, and percent relative error obtained from the independent test solutions of D-lysine and L-lysine in the validation study are summarized in Table I. Root mean square percent relative error (RMS%RE) was used to evaluate the overall prediction ability of the calibration model for the enantiomeric composition determination of lysine. The root mean square percent relative error is given by the following equation:

$$\bar{n} \quad \bar{n} \quad \bar{n} \quad \bar{n} \tag{2}$$

where $\%RE_i$ is the percent relative error determined from the known and predicted values for the ith sample in the validation set, and n is the number of validation samples in the set. From Table I, it is observed that the prediction of D-lysine (RMS%RE, 5.8%) was better than that for L-lysine (RMS%RE, 12%).

CONCLUSION

The results from the present study demonstrated a successful investigation of a chiral resorcinarene macrocycle and its selective chiral interactions with amino acid enantiomers. The chiral macrocycle had a quantum yield of 0.10, indicating relatively good fluorescence efficiency. In addition, the chiral recognition ability of the macrocycle was examined with 14 pairs of amino acid enantiomers. Examination of the results suggests that the enantiomeric selectivity of the chiral macrocycle towards lysine was highest as compared to other amino acids. Moreover, the macrocycle has potential applications for rapid screening of amino acids and can be used as an off-and-on sensor for D- and L-lysine.

ACKNOWLEDGMENTS

References

1. Buszewski B, Jezierska-Switala M, Kowalska S. J. Chromatogr. B, Anal. Technol. Biomed. Life Sci 2003;792:279.
2. Imai K, Zasshi Y. J. Pharm. Soc. Jpn 2003;123:901.
3. Onouchi H, Hasegawa T, Kashiwagi D, Ishiguro H, Maeda K, Yashima E. J. Polym. Sci. Part A: Polym. Chem 2006;44:5039.
4. Pena C, Alfonso I, Tooth B, Voelcker NH, Gotor V. J. Org. Chem 2007;72:1924. [PubMed: 17291047]
5. Ravikumar M, Prabhakar S, Vairamani M. Chem. Commun 2007:392.
6. Sheng JJ, Saxena A, Duffel MW. Drug Metab. Dispos 2004;32:559. [PubMed: 15100179]
7. Kaneko I, Yamada N, Sakuraba Y, Kamenosono M, Tutumi S. J. Neurochem 1995;65:2585. [PubMed: 7595555]
8. Powell JT, Vine N, Crossman M. Atherosclerosis 1992;97:201. [PubMed: 1466664]
9. Shapira R, Chou CHJ. Biochem. Biophys. Res. Commun 1987;146:1342. [PubMed: 2441703]

10. Armagrong DW, Gasper M, Lee SH, Zukowski J, Ercal N. Chirality 1933;5:375.

11. Lenz W. Teratology 1988;38:203. [PubMed: 3067415]

12. Slama I, Dufresne C, Jourdan E, Fahrat F, Villet A, Ravel A, Grosset C, Peyrin E. Anal. Chem 2002;74:5205. [PubMed: 12403572]

13. Paik MJ, Lee Y, Goto J, Kim KR. J. Chromatogr., B: Anal. Technol. Biomed. Life Sci 2004;803:257.

14. Matsunaga H, Sadakane Y, Haginaka J. Electrophoresis 2003;24:2442. [PubMed: 12900854]

15. Luo K, Jiang HY, You JS, Xiang QX, Guo SJ, Lan JB, Xie RG. Lett. Org. Chem 2006;3:363.

16. Yashima E, Yamamoto C, Okamoto Y. J. Am. Chem. Soc 1996;118:4036.

17. Sawada M, Takai Y, Yamada H, Nishida J, Kaneda T, Arakawa R, Okamoto M, Hirose K, Tanaka T, Naemura K. J. Chem. Soc.-Perkin Trans 1998;2:701.

18. Fakayode SO, Williams AA, Busch MA, Busch KW, Warner IM. J. Fluorescence 2006;16:659.

19. Rusin O, Alpturk O, He M, Escobedo JO, Jiang S, Dawan F, Lian K, McCarroll ME, Warner IM, Strongin RM. J. Fluorescence 2004;14:611.

20. Rusin O, Kral V, Escobedo JO, Strongin RM. Org. Lett 2004;6:1373. [PubMed: 15101745]

21. Zhu L, Zhong ZL, Anslyn EV. J. Am. Chem. Soc 2005;127:4260. [PubMed: 15783208]

22. Liu Y, Song Y, Chen Y, Li XQ, Ding F, Zhong RQ. Chem.-Eur. J 2004;10:3685.

23. Moghimi A, Maddah B, Yari A, Shamsipur M, Boostani M, Rastegar MF, Ghaderi AR. J. Mol. Struct 2005;752:68.

24. Kim JS, Quang DT. Chem. Rev 2007;107:3780. [PubMed: 17711335]

25. Lewis PT, Davis CJ, Saraiva MC, Treleaven WD, McCarley TD, Strongin RM. J. Org. Chem 1997;62:6110.

26. Timmerman P, Verboom W, Reinhoudt DN. Tetrahedron 1996;52:2663.

27. Lewis PT, Davis CJ, Cabell LA, He M, Read MW, McCarroll ME, Strongin RM. Org. Lett 2000;2:589. [PubMed: 10814385]

28. He M, Johnson RJ, Escobedo JO, Beck PA, Kim KK, Luce NN, Davis CJ, Lewis PT, Fronczek FR, Melancon BJ, Mrse AA, Treleaven WD, Strongin RM. J. Am. Chem. Soc 2002;124:5000. [PubMed: 11982364]

29. Davis CJ, Lewis PT, McCarroll ME, Read MW, Cueto R, Strongin RM. Org. Lett 1999;1:331. [PubMed: 10905872]

30. Zhang TZ, Anslyn EV. Org. Lett 2006;8:1649. [PubMed: 16597132]

31. Lin J, Li Z-B, Zhang H-C, Pu L. Tetrahedron Lett 2004;45:103.

32. Wong WL, Huang KH, Teng PF, Lee CS, Kwong HL. Chem. Commun 2004:384.

33. Wolf C, Liu SL, Reinhardt BC. Chem. Commun 2006:4242.

34. Fakayode SO, Busch MA, Bellert DJ, Busch KW. Analyst (Cambridge, U.K.) 2005;130:233.

35. Fakayode SO, Busch MA, Busch KW. Talanta 2006;68:1574. [PubMed: 18970501]

36. Tran CD, Oliveira D. Anal. Biochem 2006;356:51. [PubMed: 16860773]

37. Williams ATR, Winfield SA, Miller JN. Analyst (Cambridge, U.K.) 1983;108:1067.

38. Kirby EP, Steiner RF. J. Phys. Chem 1970;74:4480.

39. Awrich AE, Stackhouse WJ, Cantrell JE, Patterson JH, Rudman D. J. Pediatrics 1975;87:731.

40. Simell O, Perheentupa J, Rapola J, Visakorpi JK, Eskelin LE. Am. J. Med 1975;59:229. [PubMed: 1155480]

41. Flodin NW. J. Am. Coll. Nutrition 1997;16:7. [PubMed: 9013429]

42. Fakayode SO, Swamidoss IM, Busch MA, Busch KW. Talanta 2005;65:838. [PubMed: 18969877]
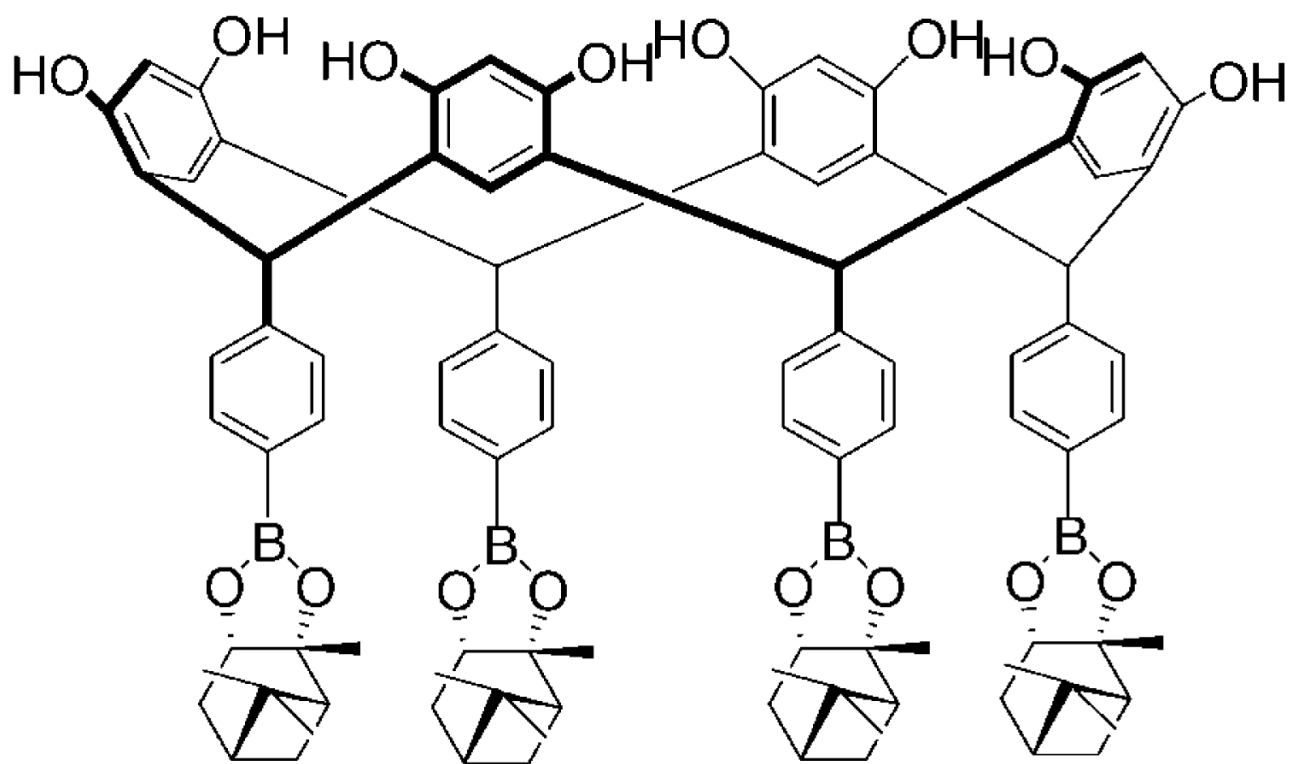
FIG. 1.
Chemical structure of tetraarylboronate resorcinarene macrocycle (TBRM).
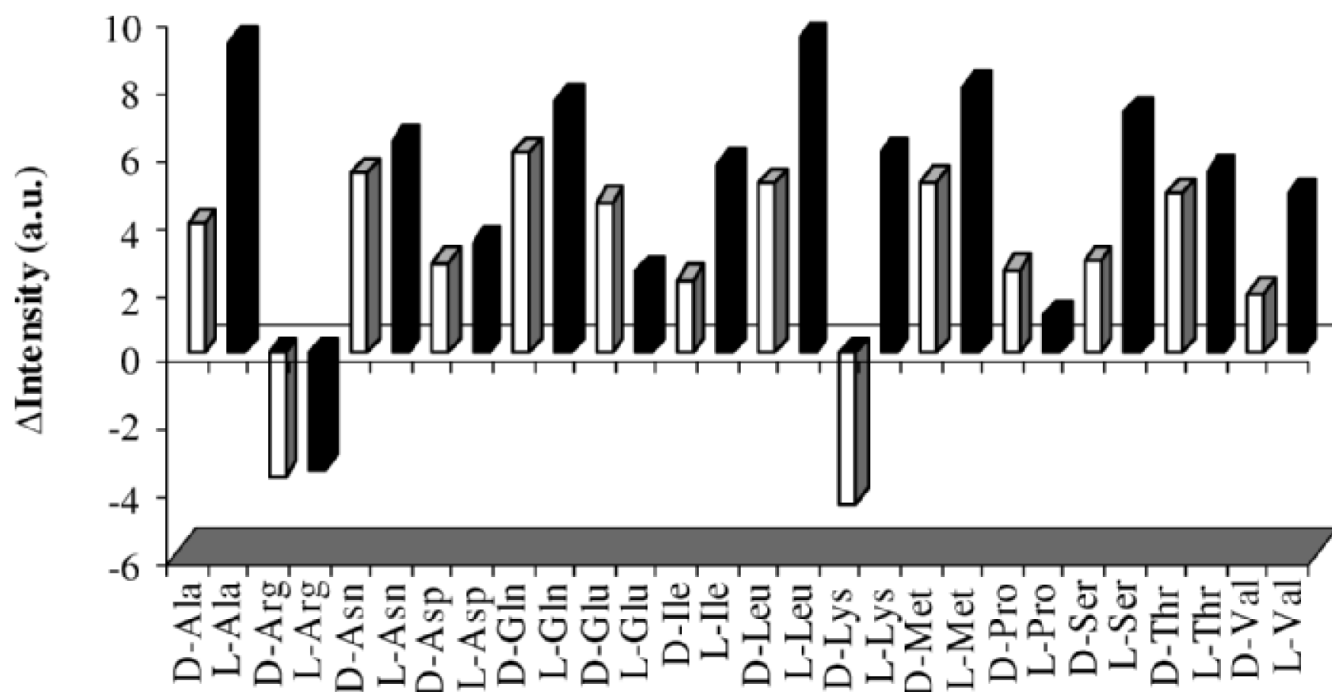
FIG. 2.
Fluorescence study of the interaction of a 7 μM TBRM with amino acids (1 mM) monitored at 435 nm emission wavelength.
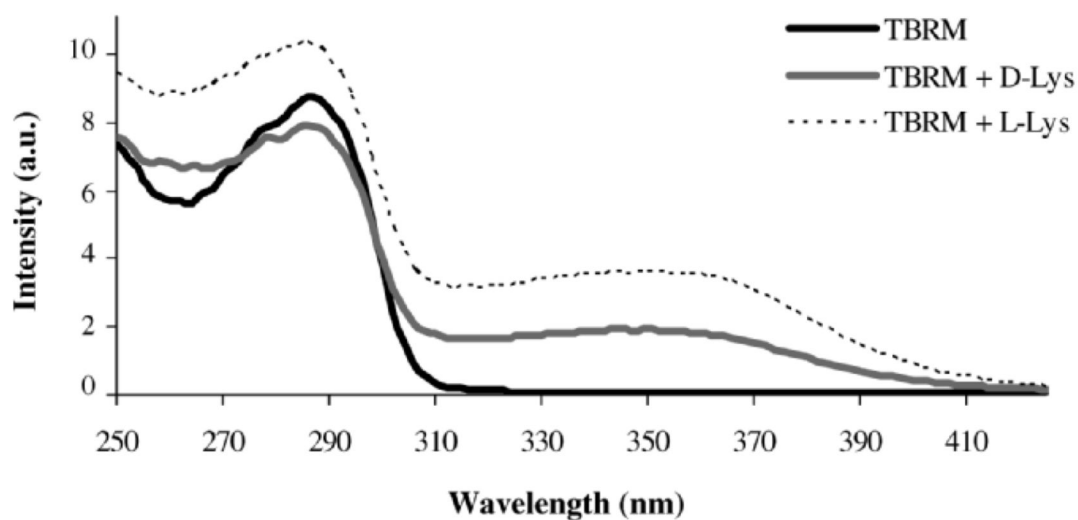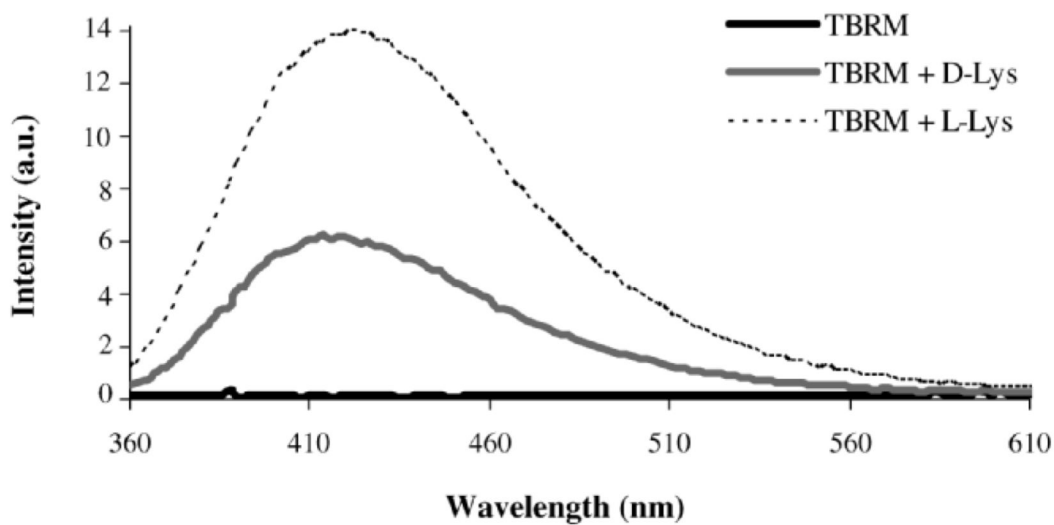
FIG. 3.
(**A**) Excitation spectra monitored at 435 nm emission wavelength and (**B**) emission spectra monitored at 350 nm excitation wavelength of TBRM (7 μM) in the absence and presence of D-lysine (1 mM) and L-lysine (1 mM).
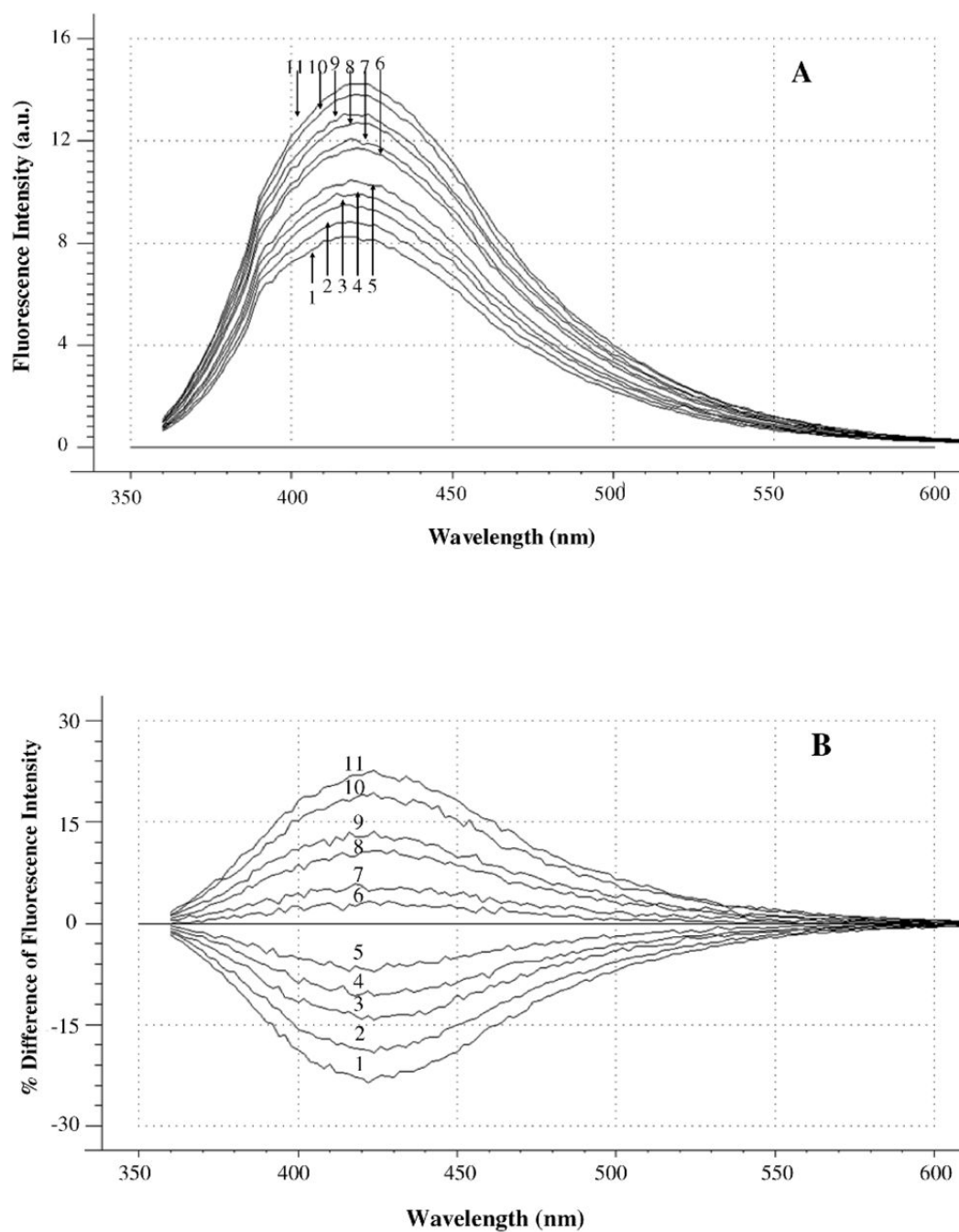
FIG. 4.
(**A**) Fluorescence spectra of 7 μM macrocycle with 2 mM lysine containing different enantiomeric compositions monitored at 350 nm excitation wavelength. The mol fraction used for L-lysine was: (**1**) 0.0, (**2**) 0.1, (**3**) 0.2, (**4**) 0.3, (**5**) 0.4, (**6**) 0.5, (**7**) 0.6, (**8**) 0.7, (**9**) 0.8, (**10**) 0.9, and (**11**) 1.0. (**B**) Mean-centered plot of 11 solutions containing the TBRM and lysine. Same mol fractions as in panel (A).

TABLE I

Actual and predicted mol fraction of D-lysine and L-lysine for solutions containing 2 mM lysine and 7 μM macrocycle.

Actual mol fraction	D-lysine predicted mol fraction	Relative error (%)	Actual mol fraction	L-lysine predicted mol fraction	Relative error (%)
0.050	0.049	1.76	0.950	0.951	-0.110
0.150	0.157	-4.67	0.850	0.843	0.820
0.250	0.230	8.00	0.750	0.770	-2.67
0.350	0.308	12.0	0.650	0.692	-6.46
0.450	0.448	0.410	0.550	0.552	-0.360
0.550	0.540	1.82	0.450	0.460	-2.22
0.650	0.589	9.38	0.350	0.411	-17.4
0.750	0.773	-3.07	0.250	0.227	9.20
0.850	0.851	-0.120	0.150	0.149	0.670
0.950	0.996	-1.68	0.050	0.034	31.6
RMS%RE		5.80	RMS%RE		12.0